Nanoscale phase changes in crystalline $Ge_2Sb_2Te_5$ films using scanning probe microscopes

H. Satoh, K. Sugawara, and K. Tanaka[a)]
Department of Applied Physics, Graduate School of Engineering, Hokkaido University, Sapporo 060-8628, Japan

(Received 2 May 2005; accepted 7 December 2005; published online 23 January 2006)

Nanoscale amorphous marks have been produced in crystalline $Ge_2Sb_2Te_5$ films using an atomic-force microscope (AFM) and a scanning-tunneling microscope (STM) through electrical phase changes. Voltage pulses with duration of 5–100 ns applied by metal probes of the AFM and the STM can produce, respectively, high-resistance regions and deformations, the smallest sizes being ~10 and ~100 nm in diameter. Raman-scattering spectra demonstrate that these marks are amorphous. The AFM mark can be erased by applying longer pulses. Formation processes of the marks are considered from electrothermal and thermodynamic aspects. © *2006 American Institute of Physics*. [DOI: 10.1063/1.2163010]

I. INTRODUCTION

Since the discovery of electrical and optical phase changes in chalcogenide glasses by Ovshinsky and coworkers,[1] the phenomena have been extensively studied from the fundamental and technological interests. At present, the optical phase change is widely commercialized as digital-versatile-disk systems,[2] in which amorphous marks are written and erased in crystalline telluride films such as $Ge_2Sb_2Te_5$ (Ref. 3) by optical heating, whereupon the marks are read as reflectivity signals using weak light.

In such a memory device, among many features, the memory capacity may be one of the most important. And, in the optical phase-change system, the capacity is in principle governed by the mark size, the smallest in the present commercial systems being ~150 nm in diameter.[4] However, this diameter is governed by the diffraction-limited spot size of blue laser light with a wavelength of 405 nm, and the ultimate material-limited size has not been known.

In previous studies,[5–8] the authors' group has demonstrated nanoscale electrical *crystallization* in amorphous $GeSb_2Te_4$ and $Ge_2Sb_2Te_5$ films using scanning probe microscopes. In the electrical phase change, which is induced by Joule heat,[1,9,10] the mark size can be reduced using smaller electrodes, for which conducting cantilevers in atomic-force microscopes (AFMs) and metal tips in scanning-tunneling microscopes (STMs) can be utilized. We could then produce crystalline marks in amorphous $Ge_2Sb_2Te_5$ films with minimal mark diameters of ~10 and ~100 nm using an AFM and a STM.[6–8] similar study has been reported also by Gidon *et al.*[11]

In the present work, we will study the reverse process; that is, electrical *amorphization* in crystalline $Ge_2Sb_2Te_5$ films, which corresponds to the mark writing process in the present optical system. This process seems to be more difficult to be induced than the crystallization, since the amorphization occurs through rapid quenching of melted $Ge_2Sb_2Te_5$, which is obtained above the melting temperature of ~600 °C,[3] which is much higher than the crystallization temperature of ~150 °C.[3] More intense Joule heating is required, which may damage microscope probes. In addition, since the amorphous state is thermodynamically quasistable,[12] smaller amorphous marks may be more fragile, which remains to be studied. It is therefore valuable to explore the ultimate mark size in the amorphization process. The present work will show that nanoscale ($\geqslant$10 nm) amorphous marks can be produced in crystalline $Ge_2Sb_2Te_5$ films. Related characteristics are considered comparatively with those of the electrical nanoscale crystallization.[5–8]

II. EXPERIMENTS

Samples employed were crystalline $Ge_2Sb_2Te_5$ films which were prepared on flat electrodes of two kinds. For the AFM experiments, the electrode was a Pt film (50 nm thick), which was sputtered onto oxide glass substrates. For STM, cleaved surfaces of highly oriented pyrolytic graphite were employed. These different electrodes were suited to different imaging methods of the two microscopes, i.e., through flowing currents in the AFM and surface topology in the STM. Nevertheless, the two electrodes did not provide essential characteristic differences. Then, $Ge_2Sb_2Te_5$ films with thicknesses of 20–500 nm were deposited using a dc sputtering apparatus with a condition previously described.[6] The films were made to crystalline $Ge_2Sb_2Te_5$ by the two procedures; one keeping the substrates at 200 °C during the film deposition, which gave clearer images for the AFM inspection with unknown reasons, and the other heating as-deposited amorphous films at 200 °C in vacuum in a sputtering chamber, which was employed mainly for the STM experiments due to better surface flatness. X-ray-diffraction patterns showed that these films had a face-centered-cubic (fcc) structure.[3] The crystallite size was estimated at ~10 nm using Scherrer's equation.

The $Ge_2Sb_2Te_5$ films were inspected and phase changed as in the previous studies.[6,7] For the AFM (SPA 300, Seiko Instruments),[7] most experiments were done using homemade Au cantilevers with a spring constant of 0.01 N/m. The

[a)]Electronic mail: keiji@eng.hokudai.ac.jp

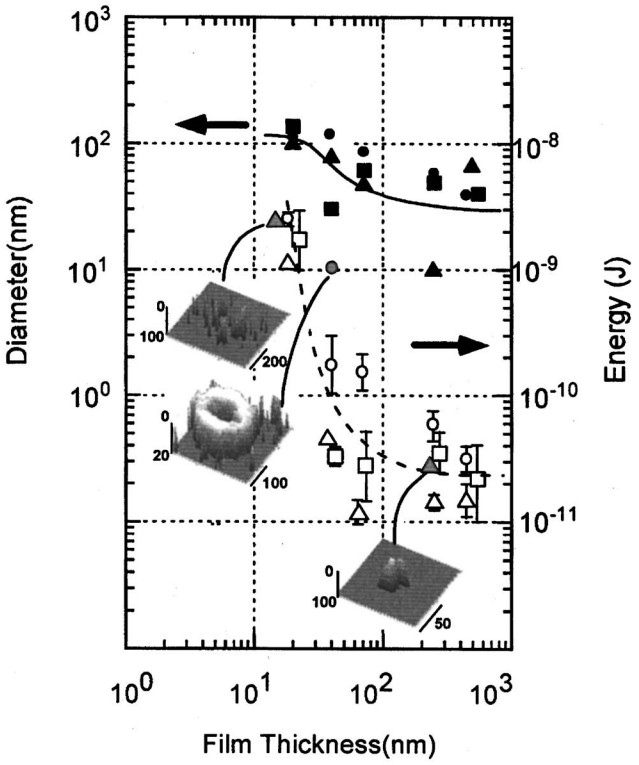

FIG. 1. Dependence of mark shape, diameter (a solid line with closed symbols with the left-hand side scale), and input energy (open symbols with the right-hand side scale) on the film thickness. The energy is calculated from a transient voltage and current wave form (see Fig. 3). The squares, triangles, and circles correspond to different pulse durations of 5, 20, and 100 ns, respectively. In the three current images, the horizontal scale is shown by the scale bar in unit of nanometer and the vertical scale varies from 20–100 nA in the background to 0 nA in the marks.

metal-coated Si_3N_4 probes previously employed for crystallization were more fragile in the present amorphization experiment. The film was covered by inactive liquid (3M, Fluorinert FC-43) for suppressing oxidation, as in the previous,[7] and it was probed as current images under a bias voltage of 10 mV. However, AFM images were sometimes blurred by stainlike grains with a typical size of ~10 nm, which limited detection of small marks. On the other hand, the STM (Nanoscope E, Digital Instruments) was operated using electrochemically polished W tips in dry air (~20% relative humidity).[6] In these two microscopes, marks were produced by applying voltage pulses with durations of 3–100 ns using two pulse generators (AVIR-1-C, AVTECH, and 214B, Hewlett Packard). For the STM, voltage pulses, which were generated in the microscope, were also employed as described later. Sample voltages and flowing currents under the applied pulses were monitored using a digital oscilloscope (54820A, Agilent Technologies). Atomic structures of produced marks were inspected using a Raman-scattering spectrometer (T64000, Jobin-Yvon) with probe light (514.5 nm and ~0.1 mW) focused to a spot of ~1 μm in diameter.

III. RESULTS

A. AFM

Figure 1 summarizes threshold features of the AFM marks as a function of the film thickness. The marks have been produced by single voltage pulses of 5 (squares), 20 (triangles), and 100 ns (circles) in duration. Longer pulses are liable to produce holes. It is mentioned that observed features do not change with the voltage polarity. In the three images, gray backgrounds correspond to currents higher than 20–100 nA, which is consistent with the electrical conductivity of $\sim 10^0$ S/cm of the crystalline $Ge_2Sb_2Te_5$,[13] and white regions correspond to smaller currents than ~0.1 nA. Such small currents and Raman-scattering spectra, described in Sec. III C, strongly suggest that the white region is amorphous.

We see that the mark shape changes with the film thickness. In the 20-nm-thick film, the mark consists of scattered stains. In the 40 nm film, ring-shaped marks tend to appear upon applications of long (20–100 ns) pulses. Simple mounds can be obtained only when the film is thicker than ~40 nm. The smallest mark obtained in the present study is the mound type with a diameter of ~10 nm, being shown in the figure, which has been produced in a 250-nm-thick film upon applying a pulse of ~30 pJ (~1.5 mW and 20 ns). However, in such nanoscales, it has been more or less difficult to distinguish a mark from background inhomogeneous stains. Accordingly, reproducible minimal marks could be ~30 nm in diameter, as shown by the solid line in Fig. 1. Nevertheless, it should be underlined that this mark size is substantially smaller than the film thicknesses of 200–500 nm, which implies that a small hemispherical mark is produced at, or near, the probe-film contact (see Fig. 8).

We also see in Fig. 1 that the mark size (solid line) and the threshold energy (dashed line) of mark formation show interesting dependence upon the film thickness. Very roughly, these values decrease in thicker films, which is in marked contrast to the increases in the mark size and the threshold voltage in the AFM crystallization.[7,8]

Figure 2 shows the mark diameter in 250-nm-thick films as functions of (a) the input power and (b) the input energy for the pulses of 5, 20, and 100 ns. Here, all the marks are the

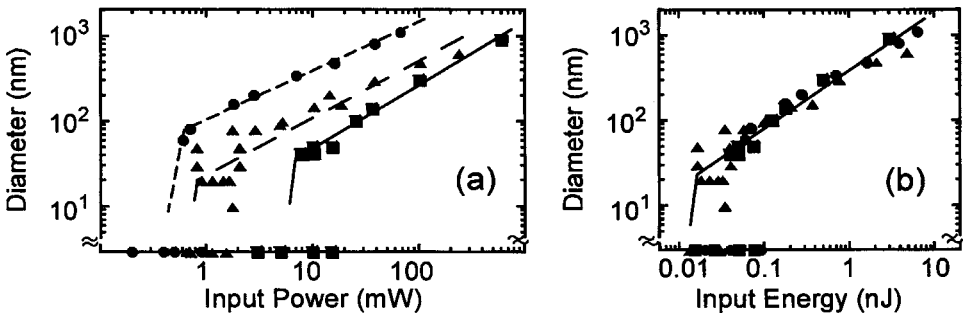

FIG. 2. Dependence of the mark diameter in 250-nm-thick $Ge_2Sb_2Te_5$ films on (a) the input power and (b) the input energy for the pulse durations of 5 ns (■), 20 ns (▲), and 100 ns (●).

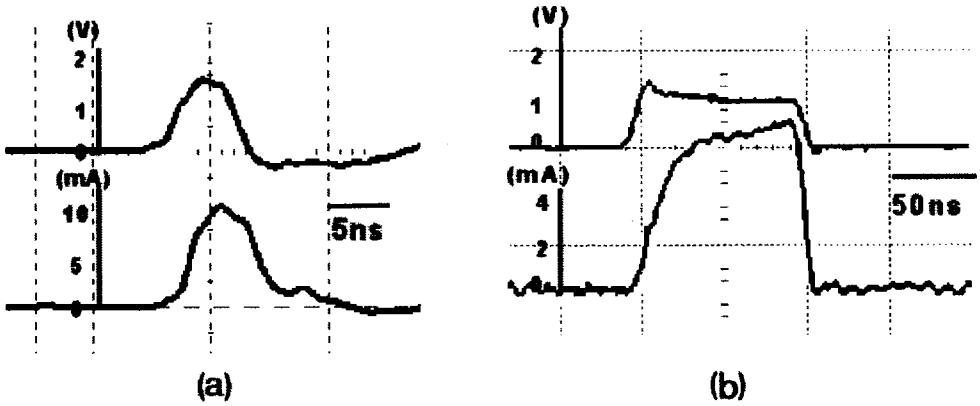

FIG. 3. Typical transients when applying a pulse of ~1 V and durations of (a) 5 ns and (b) 100 ns to a 250-nm-thick film.

mound type, while large marks with diameters of 100–1000 nm tend to accompany topological expansions lower than ~50 nm in height, which may be connected with a smaller density in amorphous states.[3,12] We see three interesting features. First, the diameter D is not determined by the input power P, but it is governed by the input energy Q as $D \propto Q^{0.5}$. Similar energy dependence has commonly been obtained for the films with thicknesses of 20, 40, 70, and 500 nm. Second, there seems to exist a threshold energy of 10–100 pJ for the mark formation, which corresponds very roughly to 1–10 mW for the pulses of 100–5 ns. Third, from (a), we can obtain $D \propto \tau^{0.5}$, where τ is the pulse duration.

Figure 3 shows typical transients obtained when applying an ~1 V pulse to a 250-nm-thick film. The 5 and the 100 ns pulse have produced a 50 and a 500 nm mark. At these short time scales, the pulse form is inevitably deformed and smoothed due to impedance mismatch and stray capacitance. In addition, the form has not been reproducible in shape, so that it cannot be closely inspected. However, we see that the form is relatively simple, being in marked contrast to the switching behavior observed in the crystallization process.[5,9,10] In addition, in the 100 ns result (b), the current tends to increase with time, which may correspond to the conductivity increase at higher temperatures in the fcc $Ge_2Sb_2Te_5$.[13]

Mark erasure has also been examined for the mound and ring types. Figure 4 shows a typical result obtained for aligned mound marks in a 250-nm-thick film. As shown in (a), six marks with a diameter of ~200 nm have been produced by short 200 pJ pulses [20 ns and ~10 mW (=1.7V $\times$7.2 mA)], and imaged. Then, (b) shows an image after the one mark has been exposed to a longer pulse of 2 V and 3 μs. This pulse has given a current of ~2 mA accompanying the so-called switching behavior, which is consistent with the crystallization process in amorphous films.[5,9,10] However, it was difficult to erase smaller marks of ~50 nm by this procedure, since the AFM drift disturbed the cantilever in accurate positioning at an amorphous mark to be erased. Then, instead of this procedure, we successively applied a short and a long pulse at a position, which produced no marks. The pulses possibly wrote and erased a mark. On the other hand, for the ring-shaped mark, the erasure was incomplete. Only a part of the ring could be erased by a single pulse under similar electrical conditions.

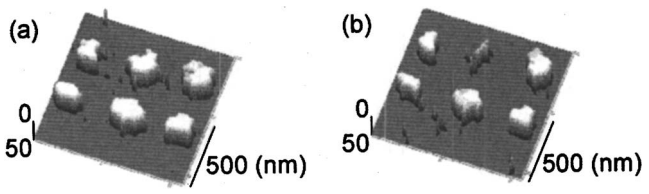

FIG. 4. (a) Six marks produced by single 20 ns pulses and (b) after an erasure by a pulse of 2 V and 3 μs.

B. STM

For the STM, since the tunneling gap must be controlled by picoampere-level currents, applications of voltage pulses to the film are more or less restricted. We have tried two methods using the internal and external pulses.

Figure 5 summarizes some results in which the pulse is generated in the microscope system.[6] In the experiment, first, the tunneling gap is adjusted by a tip voltage of −1 V and a tunneling current of 30 pA, which may fix the gap to ~1 nm. Then, under this gap condition, the voltage is increased to ±10 V, and it is held in duration of 100 μs, which is the shortest pulse duration internally generated. After that, produced marks are imaged under the initial constant-current condition, which can be regarded as giving topological images.[6] It is mentioned here that trials of detecting any electronic changes through scanning-tunneling spectroscopy, as demonstrated in the previous crystallization study,[6] have been unsuccessful. The main reason may be sought in restricted conditions in the spectroscopy measurement.

We see in Fig. 5 that the mark appears to be two kinds in shape. In the films thinner than ~50 nm, the shape is doughnutlike as shown in (a), which is similar to the crystallized STM mark in thin films of 5–50 nm [see Fig. 1(a) in Ref. 6]. On the other hand, in films thicker than ~50 nm, the shape appears to be a simple mound (b). In detail, the mound contains a dip at the center, so that the cross section is M shaped. However, the present M-shaped mound does not accompany peripheral depression, which is observed in the previous crystallized mark [see Fig. 1(b) in Ref. 6]. It should be also noted here that, in comparison with the AFM amorphization described in Sec. III A, the STM amorphization can produce many marks in reproducible shapes. Such reproducibility

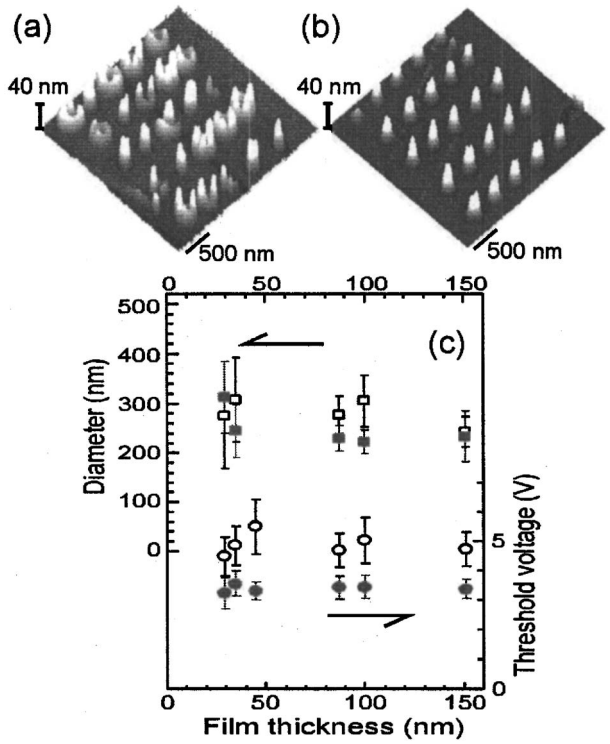

FIG. 5. STM topological images of marks produced in crystalline $Ge_2Sb_2Te_5$ films with thicknesses of (a) 35 nm and (b) 150 nm, and (c) dependence of the mark diameter (squares with the left-hand side scale) and the threshold voltage (circles with the right-hand side scale) on the film thickness. The open and closed symbols indicate the positive and negative tip voltages. Each point represents ~50 data, and the error bars show rms deviations.

seems to be due to the tip made from W, which is harder than Au, which has been employed for the AFM cantilevers because of needed flexibility.

Dependence of the mark diameter and the threshold voltage upon film thickness (30–150 nm) is interesting. Very roughly, the present amorphization does not show prominent thickness dependence. In detail, the mark diameter (200–300 nm) tends to decrease in thicker films, and the threshold voltage shows polarity dependence, 3–4 V for the negative and 4–5 V for the positive. These features are contrastive to those in the crystallization, in which the mark diameter and the threshold voltage have monotonically increased from 100 to 500 nm and from 3 to 9 V with a film-thickness increase from 1 to 150 nm.[6,8] In addition, no polarity dependence appeared.

It should be noted that the mark diameter and the threshold voltage have not changed when the pulse duration is lengthened to 1 ms. Such a feature on the pulse duration has also been found in the previous crystallization experiment,[6] which has been ascribed to a unique transient characteristic (see Fig. 3 in Ref. 6). That is, the internal voltage pulse rises at a rate of 10 V/5 μs, which is limited by the STM,[6] and when it reaches to the threshold of 3–5 V in the present experiment, a current spike of 1–2 mA flows only in duration of ~20 ns, which is governed by a time constant of STM feedback loop.[6] Applied pulses are much longer than this, and accordingly, no pulse-duration dependence can appear.[14]

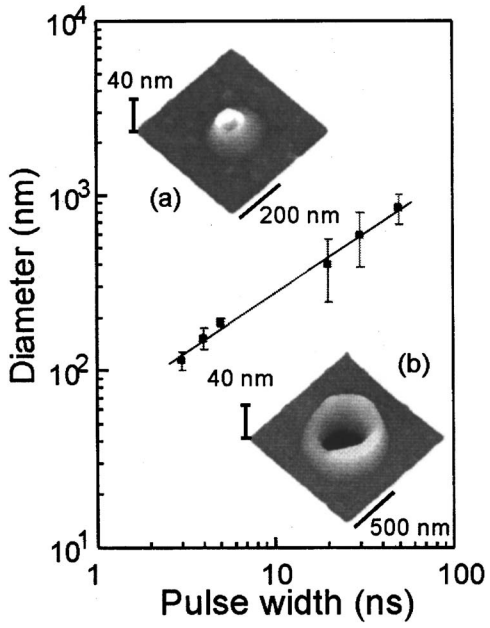

FIG. 6. Mark diameter as a function of pulse duration in a 100-nm-thick film. Each point represents an average of 10–50 data, and the error bars show rms deviations. STM topological images of marks produced by (a) a 5 ns and (b) a 50 ns pulse are also included.

To examine pulse-duration dependence, therefore, we have modified the STM so that external pulses can be applied to a sample. For this purpose, two electric relays (Omron, G6Y) were used to change a tip-sample circuit from an internal STM bias supply to an external pulse generator, which could provide short pulses to the film.

Figure 6 shows some results, in which a 100-nm-thick film is subjected to single –5 V pulses. The result manifests clear pulse-duration dependence of $D \propto \tau^{0.7}$. We see in (a) that a 5 ns pulse produces an M-shaped mound with a height of ~10 nm and diameter of ~100 nm. Longer pulses such as 50 ns produce clear doughnutlike marks, as exemplified in (b). In this short pulse experiment, specifically when a pulse was shorter than ~10 ns, accurate current transients could not be monitored due to stray capacitance and so forth, while the peak values appeared to be ~10 mA.

C. Raman-scattering spectroscopy

The marks produced by the AFM and STM have been demonstrated to be amorphous by Raman-scattering spectroscopy. Figure 7(a) is a spectrum obtained for an as-sputtered film. The broad peak at ~150 cm^{-1}, which is a signature of an amorphous structure, is assigned to a Te–Te stretching mode.[15] In contrast, a fcc film (c) does not show any clear peak, which is also consistent with the previous study.[15] Origins of the broad step at a small wave number are speculative.[16] On the other hand, as exemplified in (b), the mound-type AFM mark (see Fig. 1) and all the STM marks provide the peak at 150 cm^{-1}. That is, these marks are amorphous, which strongly suggests that a phase change from the crystalline phase to the amorphous state is induced by voltage pulses.

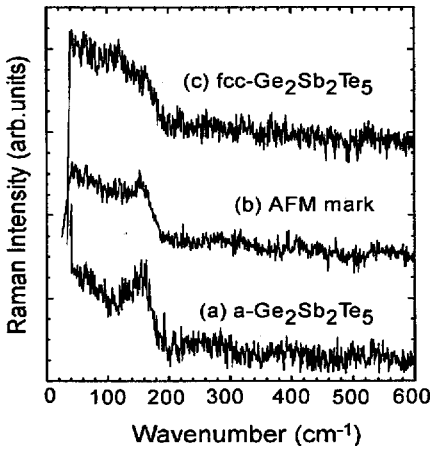

FIG. 7. Raman-scattering spectra of (a) an as-deposited amorphous state, (b) an AFM mound-shaped mark with a diameter of ~ 1 μm, and (c) a fcc phase in a 250-nm-thick film.

For the ring-shaped AFM mark (see Fig. 1), however, the Raman peak at 150 cm^{-1} could not be detected. This is probably due to the ring area which is much smaller than the probe light diameter of ~ 1 μm.

IV. DISCUSSION

A. Overall features

In general, the amorphization can occur through rapid quenching of melts.[12] In the AFM experiment, when applying a voltage pulse, reflecting a centrifugal electric field emerging from a point contact between an AFM cantilever and a crystalline $Ge_2Sb_2Te_5$ film, Joule heating starts to occur. The heated region probably extends with increasing input energy, and if the temperature reaches to the melting point of $\sim 600\,^{\circ}C$,[3] the region will melt. Then, after the pulse cessation, the melt rapidly cools down through heat dissipation into the cantilever and a lower electrode, and finally it may be converted to an amorphous mark. These processes will produce hemispherical marks near the film surface, if the mark radius is smaller than the film thickness.

On the other hand, in the STM, the existence of tunneling gaps makes the process more complicated. The previous work suggests that nanoampere-level tunneling currents cannot melt $Ge_2Sb_2Te_5$.[8] Alternatively, application of voltage pulses of ~ 3 V to a tunneling gap causes elongation of a STM tip by ~ 10 nm due to Coulombic attraction,[6] and in consequence the STM tip makes an electrical contact with the $Ge_2Sb_2Te_5$ film. The central dips of STM marks, observed in Figs. 5 and 6, are assumed to be traces of this tip insertion.[6,8] The contact can then conduct a high current, so that a process occurring after the tip insertion becomes to be the same as the AFM case. Nevertheless, since the higher voltage (3–5 V) is applied directly to the sample, the mark necessarily becomes to be larger than that in the AFM experiment (~ 1 V).

From these models, we may have several subjects to be studied. What is a maximal temperature generated in the film by an electrical input? How can we interpret the minimal mark size of ~ 10 nm? Why does the amorphization exhibit contrastive film-thickness dependence to that in the crystallization? In the following, we will consider these problems, focusing upon the simple mound-shaped marks obtained in the AFM and STM experiments.

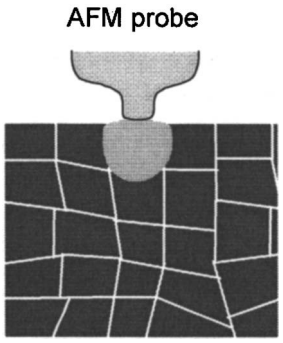

FIG. 8. A cross-sectional view of an amorphous mark produced by a voltage pulse applied from an AFM probe to a crystalline $Ge_2Sb_2Te_5$ film. The crystallite size is assumed to be ~ 10 nm.

B. Temperature rise

Estimation of temperature rise is not straightforward, since the rise occurs transiently in nanometer scales. Here, we write very roughly a spatially averaged temperature rise ΔT in a crystalline $Ge_2Sb_2Te_5$ film at a steady state as

$$Q_{\text{in}} - Q_{\text{out}} = CV\Delta T, \tag{1}$$

where Q_{in} is the input electrical energy, Q_{out} represents heat dissipation into a microscope probe, i.e., an AFM cantilever or a contacted STM tip, C the specific heat of $Ge_2Sb_2Te_5$,[17,18] and V a heated volume. We here neglect the substrate, since the thermal diffusion length L_t ($=40-200$ nm) is comparable or smaller than the film thickness (200–500 nm) of interest. Note that $L_t \approx (\kappa\tau)^{1/2}$, where κ is the thermal conductivity (~ 0.5 W/m K) (Ref. 17) in $Ge_2Sb_2Te_5$ and τ ($=5-100$ ns) is the pulse duration. In Eq. (1), Q_{in} can be estimated straightforwardly from an applied voltage, a flowing current, and the pulse duration. The heated volume V is assumed to be hemispherical, which can be written as $V \approx 2\pi L_t^3/3$. On the other hand, to calculate Q_{out}, we assume that the probe apex has a cylinder shape with a length L and a contact area of S, and the root is connected to a thick rod, which can be regarded as a heat bath (see Fig. 8). Actually, observations using a high-resolution scanning-electron microscope have obtained such images with typical dimensions of $L \approx 10$ nm and $S \approx 5^2\pi$ nm^2. Then, we can write down as $Q_{\text{out}} = \tau\kappa_p S\Delta T/L$, where κ_p (~ 100 W/m K) (Ref. 19) is the thermal conductivity of the probe metal. Finally, a simple calculation using material constants[17–19] shows $CV\Delta T \ll Q_{\text{out}}$ and $\Delta T[\text{K}] \approx 4 \times 10^5 P[\text{W}]$.

This result may be employed as a tentative for examining the two important observations. First, the equation suggests that the temperature rise ΔT is governed by the input power P, and that the melting temperature of $\sim 600\,^{\circ}C$ is attained at $P \approx 1.5$ mW. This power is comparable to the threshold power of 1–10 mW shown in Fig. 2(a). However, as we have seen in Fig. 2(b), the threshold appears to be governed by the input energy Q_{in}, not by the power P. Such a disagreement may be inevitable in the present rough analy-

sis, because as we have seen in Fig. 3 P and Q_{in} cannot be evaluated accurately for the short pulses due to pulse deformations and so forth. Second, the radius L_t of heated volumes is predicted to increase in proportion to $\tau^{0.5}$, so that the mark diameter D possibly has similar τ dependence, which is consistent with the AFM result, $D \propto \tau^{0.5}$ [Fig. 2(a)], and resembles the STM result, $D \propto \tau^{0.7}$ (Fig. 6). However, it seems to be difficult to explain the simple observation of $D \propto Q^{0.5} \propto P^{0.5}$ in Fig. 2. To get deeper insight, we should know cross-sectional mark shapes. In addition, we should also know a role of latent heat at the melting, which is neglected in the above analysis. It may be plausible that, when the electrical power is greater than the threshold, the sample temperature is still held at the melting temperature due to the latent heat. Alternatively, superheating may occur on the present time scale of 5–100 ns.

C. Minimal mark size

We here consider the reason why we cannot produce smaller marks than ~10 nm. At least, two possibilities can be proposed.

One is that the mark size may be governed by the probe dimension. Since the minimal size of ~10 nm has appeared also in the crystallization,[7,8] the probe dimension may commonly be decisive in the mark sizes. In detail, mark production and/or detection could be governed by the apex size of the AFM cantilevers.

The other is a thermodynamical model. The idea has been employed previously for understanding the minimal size of crystalline marks.[8] However, the model cannot be applied here in its original form, since an amorphous state is less stable than a crystalline phase ($\Delta G_A > 0$). Then, recalling that the crystallite size of the present film is ~10 nm, as mentioned in Sec. II, which is comparable to the minimal mark size, we write the free-energy change ΔG for amorphization, taking boundary energies into account, as

$$\Delta G = \Delta G_A + \Delta G_{AC} - \Delta G_{CC}, \tag{2}$$

where $\Delta G_A (>0)$ represents an amorphous energy relative to that in the crystalline phase,[8] ΔG_{AC} an amorphous-crystalline boundary energy, and ΔG_{CC} a crystalline-crystalline boundary energy. Here, if a crystallite is converted to an amorphous mark, as illustrated in Fig. 8, $\Delta G_{AC} - \Delta G_{CC}$ could be negative as suggested theoretically for Si.[20] Such a situation can provide a minimum for ΔG at the corresponding size. That is, the amorphous mark could exist in quasistable, if the size is similar to the crystallite size (or its multiples). The minimal mark size can therefore be comparable to the crystallite size, ~10 nm, irrespective of the film thickness. Note that this idea is contrastive to the thermodynamic interpretation on the crystalline-mark formation, in which the minimal radius is assumed to be the same as the film thickness.[8]

At present, it is difficult to conclude which model is more plausible. To examine the first model, we have done some experiments using metal-coated Si_3N_4 probes, which could produce smaller crystalline marks in the previous study.[7] However, the minimal size of amorphous marks was comparable to that produced by the Au probe. On the other hand, to examine the second model, we have tried to prepare crystalline films having different crystallite sizes under varied heat-treatment conditions. However, the trial has not succeeded. For instance, annealing of sputtered $Ge_2Sb_2Te_5$ films at a higher temperature (~270 °C) caused thermal reaction between the film and the bottom Pt electrode.

D. Film-thickness dependence

As pointed out in Secs. III A and III B, the present amorphization experiment has provided contrastive film-thickness dependence to that of the crystallization. Roughly, in the present case, the minimal mark size and the threshold decrease (Fig. 1) or hardly change (Fig. 5) with an increase in the film thickness; while by contrast, these values clearly increase in the crystallization.[6–8] This difference can be ascribed to different dominant factors.

For the crystallization in an amorphous film, which is substantially insulating ($\sim 10^{-4}$ S/cm),[13] an electrically conducting channel must be formed at the outset.[8–10] The formation threshold is governed by the applied electric field,[9,10] which requires higher voltages in thicker films. Accordingly, the threshold voltage increases with the thickness, e.g., from 4 to 20 V for the AFM.[7,8] On the other hand, the minimal mark size is governed by the film thickness,[8] because of the endothermic crystallization reaction and so forth, so that the size also increases with the film thickness.

The amorphization in crystalline films is contrastive. Since the crystalline film is substantially conductive ($\sim 10^{0}$ S/cm),[13] a current can flow under a low voltage, and Joule heat is generated at, or near, the probe-film contact. Since the melting temperature is high (~600 °C) and the thermal conductivity (~100 W/m K) (Ref. 19) of the bottom electrode is much higher than that (~0.5 W/m K) (Ref. 17) of $Ge_2Sb_2Te_5$, Joule heating at (near) the probe-film contact is more efficient in thicker films. This thermal situation possibly governs the decrease in the AFM threshold energy with an increase in the film thickness. The energy decrease is also favorable to the reduction in the mark size (Fig. 1). On the other hand, in the STM, the threshold voltage is governed by the tip elongation as described in Sec. IV A. Accordingly, the small resistance of crystalline films can be neglected, and the threshold voltage is nearly independent of the film thickness. However, further studies are needed for other observations such as the polarity dependence shown in Fig. 5.

V. SUMMARY

Nanoscale amorphization in crystalline $Ge_2Sb_2Te_5$ films has been demonstrated using an AFM and a STM. Pulsed voltages with duration of 5–100 ns can produce amorphous marks, which are confirmed using Raman-scattering spectroscopy. The minimal mark sizes are ~10 nm for the AFM and ~100 nm for the STM. The AFM marks can be erased by applying longer pulses. In the amorphization, the mark size and the threshold input for mark formation tend to decrease in thicker films. These characteristics are considered comparatively with those in the nanoscale crystallization.

Finally, it may be valuable to mention that the 10 nm mark is capable to produce, under a simple extrapolation,

terabyte memories. This capacity is greater by two orders than the present highest disk capacity of 50 GB.[4]

ACKNOWLEDGMENTS

The authors would like to thank Dr. T. Gotoh for continuous supports and Mr. T. Ryoke for preliminary experiments.

[1]S. R. Ovshinsky and H. Fritzsche, IEEE Trans. Electron Devices **ED-20**, 91 (1973).
[2]T. Ohta and S. R. Ovshinsky, *Photo-Induced Metastability in Amorphous Semiconductors*, edited by A. V. Kolobov (Wiley-VCH, Weinheim, 2003), Chap. 18.
[3]N. Yamada, E. Ohno, K. Nishiuchi, N. Akahira, and M. Takao, J. Appl. Phys. **69**, 2849 (1991).
[4]T. Nishihara, R. Kojima, N. Miyagawa, and N. Yamada, Jpn. J. Appl. Phys., Part 1 **44**, 3037 (2005).
[5]T. Gotoh, K. Sugawara, and K. Tanaka, J. Non-Cryst. Solids **299-302**, 968 (2002).
[6]K. Sugawara, T. Gotoh, and K. Tanaka, Jpn. J. Appl. Phys., Part 2 **43**, L676 (2004).
[7]T. Gotoh, K. Sugawara, and K. Tanaka, Jpn. J. Appl. Phys., Part 2 **43**, L818 (2004).
[8]K. Tanaka, T. Gotoh, and K. Sugawara, J. Optoelectron. Adv. Mater. **6**, 1133 (2004).
[9]A. Madam and M. P. Shaw, *The Physics and Applications of Amorphous Semiconductors* (Academic, Boston, 1988), Chap. 5.
[10]A. Pirovano, A. L. Lacaita, A. Benvenuti, F. Pellizzer, and R. Bez, IEEE Trans. Electron Devices **51**, 452 (2004).
[11]S. Gidon, O. Lemonnier, B. Rolland, O. Bichet, and C. Dressler, Appl. Phys. Lett. **85**, 6392 (2004).
[12]S. R. Elliott, *Physics of Amorphous Materials*, 2nd ed. (Longman Scientific & Technical, Essex, 1990).
[13]I. Friedrich, V. Weidenhof, W. Njoroge, P. Franz, and M. Wuttig, J. Appl. Phys. **87**, 4130 (2000).
[14]In detail, however, a noisy current before the current spike, shown in the previous (Ref. 6), does not appear in the present experiment.
[15]J. Tominaga and N. Atoda, Jpn. J. Appl. Phys., Part 2 **38**, L322 (1999).
[16]A. V Kolobov, P. Fons, A. I. Frenkel, A. L. Ankudinov, J. Tominaga, and T. Uruga, Nat. Mater. **3**, 703 (2004).
[17]P. K. Khulbe, E. M. Wright, and M. Mconsuripur, J. Appl. Phys. **88**, 3926 (2000).
[18]W. K. Njoroge, H.-W. Woltgens, and M. Wuttig, J. Vac. Sci. Technol. A **304/306**, 73 (2001).
[19]*Handbook of Chemistry and Physics*, 74th ed., edited by D. R. Lide (CRC, Boca Raton, 1993), Chap. 12.
[20]S. Izumi, S. Hara, T. Kumagai, and S. Sakai, Comput. Mater. Sci. **31**, 279 (2004).